Original article

Corydalis Rhizoma as a model for herb-derived trace metabolites exploration: A cross-mapping strategy involving multiple doses and samples

Chanjuan Yu [a],[1], Fengyun Wang [b],[1], Xinyue Liu [a], Jiayan Miao [a], Siqi Tang [a], Qin Jiang [a], Xudong Tang [b],[**], Xiaoyan Gao [a],[*]

[a] School of Chinese Materia Medica, Beijing University of Chinese Medicine, Beijing, 102488, PR China
[b] Gastroenterology Department, Xiyuan Hospital, China Academy of Chinese Medical Sciences, Beijing, 100091, PR China

A B S T R A C T

Deciphering the metabolites of multiple components in herbal medicine has far-reaching significance for revealing pharmacodynamic ingredients. However, most chemical components of herbal medicine are secondary metabolites with low content whose in vivo metabolites are close to trace amounts, making it difficult to achieve comprehensive detection and identification. In this paper, an efficient strategy was proposed: herb-derived metabolites were predicted according to the structural characteristics and metabolic reactions of chemical constituents in Corydalis Rhizoma and chemical structure screening tables for metabolites were conducted. The fragmentation patterns were summarized from representative standards combining with specific cleavage behaviors to deduce structures of metabolites. Ion abundance plays an important role in compound identification, and high ion abundance can improve identification accuracy. The types of metabolites in different biological samples were very similar, but their ion abundance might be different. Therefore, for trace metabolites in biological samples, we used the following two methods to process: metabolites of high dose herbal extract were analyzed to characterize those of clinical dose herbal extracts in the same biological samples; cross-mapping of different biological samples was applied to identify trace metabolites based on the fact that a metabolite has different ion abundance in different biological samples. Compared with not using this strategy, 44 more metabolites of clinical dose herbal extract were detected. This study improved the depth, breadth, and accuracy of current methods for herb-derived metabolites characterization.

1. Introduction

It is generally believed that the components of drugs absorbed into the body and related metabolites are the effective material basis for disease treatment [1–3]. Compounds in herbal medicines that vary significantly in structural types and contents lead to more complex metabolome after metabolism in vivo. Moreover, the matrix of biological samples is complex, and some high-content or high-response endogenous substances may interact with drug metabolites, resulting in ion inhibition or enhancement, which interferes with the detection of herb-derived metabolites. All these factors pose a serious challenge for global detection and accurate identification of in vivo herb-derived metabolites.

In view of difficulties mentioned above in metabolic studies, more and more techniques have been employed to detect and characterize in vivo metabolites. With a view to improving detection sensitivity, some techniques based on mass spectrometry (MS) data such as mass defect filter [4], background subtraction [4,5], characteristic ions filtering and neutral loss filtering [6–8] were proposed. But these techniques might miss metabolites with inconspicuous chromatographic peaks whose MS/MS information is missing or submerged at the baseline. As a complement, multivariate statistical analysis [9] was applied to ensure the comprehensiveness of metabolite detection. The low sensitivity limited its application.

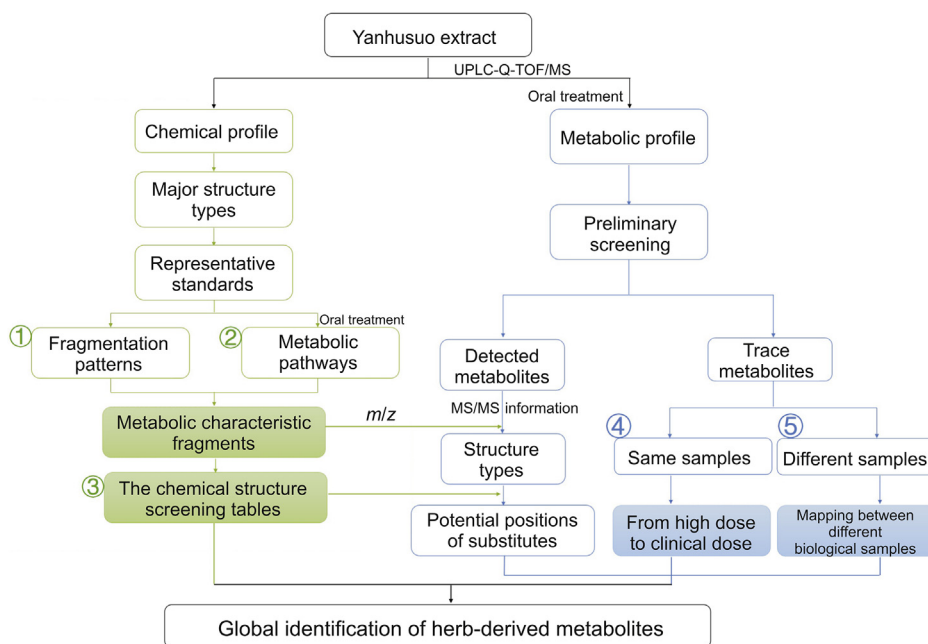As for structure characterization accuracy, the structures of

Fig. 1. Summary diagram of proposed analytical strategy for identification of Yanhusuo alkaloids metabolites.

metabolites were only confirmed by comparison with reference standards in previous reports. The other metabolites without standards were characterized by metabolic pathways and fragmentation patterns, and their structures were represented by the parent drugs and related metabolic reactions.

There is an urgent need for an effective method for detection and identification of metabolites. Therefore, in this study cross-mapping of different doses and samples was used for trace metabolites detection. The chemical structure screening tables and characteristic fragments were combined to enhance the accuracy of metabolite structure identification.

The dry rhizoma of *Corydalis yanhusuo* W.T. Wang (Papaveraceae) (Yanhusuo in Chinese) has the effect of promoting blood circulation, promoting qi and relieving pain [10]. Due to its strong physiological effects, more and more research on Yanhusuo has been carried out in recent years. Previous studies only showed metabolic pathways and metabolites of certain components like tetrahydropalmatine [11,12], corydaline [13,14], dehydrocorydalis [15] and palmatine [16]. Few studies focused on the comprehensive metabolic profile of Yanhusuo alkaloids, and metabolites were not fully discovered because of the inherent limitation of analytical methods [17]. Through preliminary study of chemical constituents, we had a comprehensive understanding for Yanhusuo alkaloids [18]. However, the pharmacodynamic constituents of Yanhusuo are still not clear.

Herein, Yanhusuo was selected as the model herb to establish a strategy for herb-derived metabolites characterization in this study. The strategy mainly included the following steps. First, representative authentic standards of homologous components contained in Yanhusuo were chosen, from which the fragmentation patterns were proposed. Second, the metabolic pathways and metabolic characteristic fragments (MCFs) of each family of compounds were acquired through metabolic analysis of standards. Third, the structure screening tables established on the basis of the structural characteristics and metabolic pathways of compounds in Yanhusuo were combined with fragmentation patterns and MS information to

characterize structures of metabolites. Then, metabolites of high-dose extract were used as pseudo-standard to identify those of clinical dose so as to identify metabolites with low ion abundance in the same biological samples. Finally, cross-mapping of different biological samples was applied to identify trace metabolites in different samples.

A total of 127 herb-derived metabolites were identified in biological samples after the clinical dose Yanhusuo administration. For the first time, the metabolite structures of four standards representing Yanhusuo alkaloids were clearly characterized, and metabolic pathways were proposed based on this. The strategy provided a reference for pharmacodynamic substances discovery in different biological samples and metabolism mechanism of TCMs. The specific workflow is shown in Fig. 1.

2. Materials and methods

2.1. Chemicals and reagents

Herbal materials of Yanhusuo were purchased from Beijing Tong Ren Tang Group Co., Ltd. (Beijing, China) and identified by Professor Yaojun Yang, School of Chinese Materia Medica, Beijing University of Chinese Medicine. The voucher specimens were deposited in School of Chinese Materia Medica, Beijing University of Chinese Medicine, China. Protopine, tetrahydropalmatine, tetrahydroberberine and palmatine with purity of above 98% were obtained from Chengdu Biopurify Phytochemicals Ltd. (Chengdu, China). Liquid chromatography coupled with mass spectrometry (LC-MS) grade acetonitrile, methanol, and formic acid were purchased from Fisher Scientific (Fisher, Fair Lawn, NJ, USA). Distilled water was available from the A.S. Watson Group Ltd. (Hong Kong, China).

2.2. Animals

Male Sprague-Dawley rats ((200 ± 10) g) were purchased from
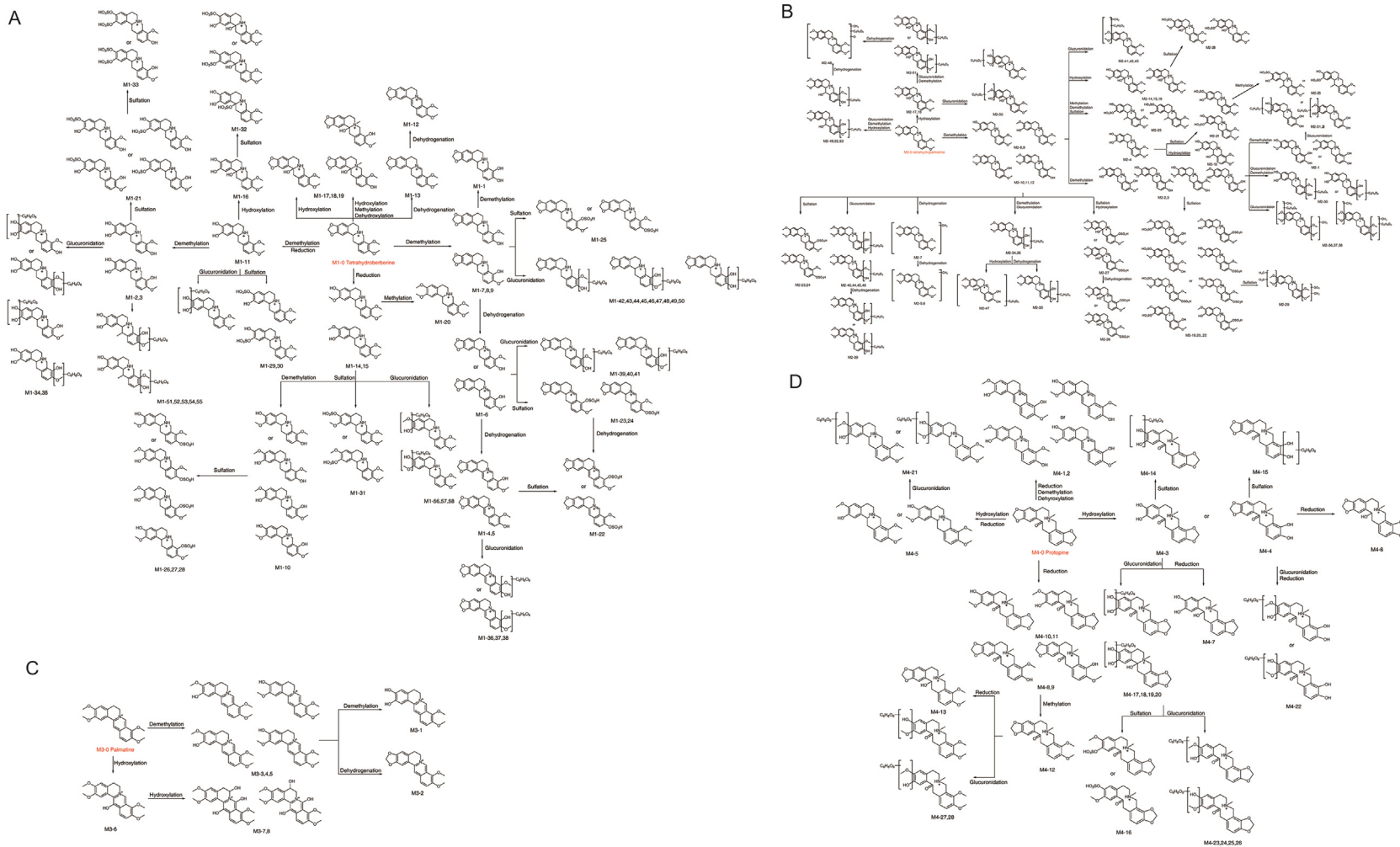
Fig. 2. Proposed metabolic pathway of tetrahydroberberine (A), tetrahydropalmatine (B), palmatine (C), and protopine (D).

Beijing Weitong Lihua Biotechnology Co., Ltd. (Beijing, China). All the rats were kept under controlled environmental conditions (a 12 h light/12 h dark cycle, a temperature of $(20 \pm 2)\,°C$ and humidity of $(60 \pm 5)\%$ with free access to food and water for three days before the experiments. All animal experiments were approved by the Animal Ethics Committee of Beijing University of Chinese Medicine (Beijing, China), and all procedures were performed in accordance with the Helsinki Declaration.

Then rats were randomly divided into 3 groups: the feces and urine group ($n = 12$), the plasma group ($n = 12$) and the bile group ($n = 14$). The rats in the feces and urine group were divided into 6 groups and were orally administered four reference standards (2.00 mL), clinical dose (0.56 mL) and high dose (1.20 mL) of Yanhusuo extract, respectively. The feces and urine samples of 12 rats were collected for 24 h before and after administration, respectively. The urine samples were centrifuged at 12,000 rpm for 15 min and the supernatant was frozen in a refrigerator at $-80\,°C$. The feces samples were placed in a fume hood for drying. Then dried feces were crushed and stored in a centrifuge tube at $-80\,°C$. The other two groups used the same drugs and method of administration, except for the bile group, which had two more rats for blank control. Blood samples of 0.5 mL were collected via the ophthalmic veins into heparinized tubes at 0 and 5, 10, 30, 45, 60, 120, 180, 240, 360, 480, 600, 720 min after the administration. The samples were centrifuged at 3,500 rpm and $4\,°C$ for 15 min. Rats in the bile group were anesthetized by 10% chloral hydrate for bile duct intubation. The bile samples were collected for 0—12 h and 12—24 h, and stored at $-80\,°C$.

2.3. Sample preparation

2.3.1. Sample preparation of Yanhusuo extract and standards

The standard solutions of four reference standards were prepared in 0.5% aqueous solution of sodium carboxymethyl cellulose at a concentration of 2 mg/mL. Intragastrical administration dose of each standard solution was 20 mg/kg, i.e., 2 mL per rat.

Herbal materials of Yanhusuo were powdered by a grinder and sieved through a 40-mesh sieve. About 20 g of powder was soaked in 200 mL of distilled water for 1 h and decocted twice by boiling, each time for 30 min. Then, extracting solution was merged and drained with a water bath. The residue was dissolved in 40 mL of distilled water and configured to be a concentration which was equivalent to 0.5 g of herbal materials (The oral clinical dosage of Yanhusuo in the Chinese Pharmacopoeia is 3—10 g for per person. So, the clinical dosage of Yanhusuo is 1.4 g/kg, which is 0.28 g per rat (0.56 mL). The high dosage was 3 g/kg, which was 0.6 g per rat (1.2 mL)). The extract was stored at $-4\,°C$.

2.3.2. Blood, urine and bile samples preparation

The frozen samples were dissolved at room temperature. 200 μL of plasma sample from each time point was mixed. An appropriate amount of mixed sample (100 μL for plasma sample, 1 mL for urine sample and 150 μL for bile sample) was mixed with three times amount of methanol in polypropylene test tube. Then the mixture was vortex-mixed for 30 s and centrifuged at 12,000 rpm and $4\,°C$ for 10 min to remove the precipitated protein. The supernatants were dried with nitrogen. The residue was re-dissolved with 100 μL of 70% methanol and then centrifuged at 12,000 rpm and $4\,°C$ for 15 min. The supernatants were subjected to ultra-performance liquid chromatography coupled with quadrupole time of flight tandem mass spectrometry (UPLC-Q-TOF/MS) system.

2.3.3. Feces samples preparation

200 mg feces were vortexed in 4 mL of methanol for 30 s and placed for 1 h. Then the suspensions were centrifuged at 12,000 rpm and $4\,°C$ for 15 min. The supernatants were dried with nitrogen. The residue was re-dissolved with methanol, and then centrifuged at 12,000 rpm and $4\,°C$ for 15 min. The supernatants were subjected to UPLC-Q-TOF/MS system.

2.4. Instrumentation and conditions

The LC analysis was carried out on Waters ACQUITYTM UPLC I - Class system (Waters, Milford, MA, USA) consisting of a binary solvent system, an autosampler and a column temperature controller. The system was operated under MassLynx V4.1 software (Waters, Milford, MA, USA). The chromatographic separation was carried out on an ACQUITY BEH C_{18} column (2.1 mm × 100 mm, 1.7 μm, Waters, Ireland). The mobile phase was composed of eluent A (0.1% formic acid in water) and eluent B (acetonitrile). The line gradient program was optimized as follows: 0—2 min, 1%—10% B; 2—15 min, 10%—20% B; 15—22 min, 20%—30% B; 22—27 min, 30%—90% B; 27—29 min, 90% B; 29—29.1 min, 90%—2% B; and 29.1—31 min, 2%—2% B. The column temperature was set at $40\,°C$. The sample chamber temperature was set at $4\,°C$. The mobile phase flow rate was set at 0.3 mL/min, and the injection volume was 2 μL for each run.

The MS analysis was carried out by a Waters SYNAPT G2-SI MS system (Waters, Manchester, UK) equipped with electrospray ionization. The analysis was performed in the positive ion electrospray mode, and the source parameters were set as follows: the capillary voltage was 3.0 kV and the cone voltage was set at 40 V; the source temperature was $100\,°C$, and the desolvation gas temperature was $400\,°C$; the cone gas flow was 50 L/h, and the desolvation gas flow was 800 L/h; the low collision energy was 6 eV, and the high collision energy was 10—40 eV. The scan range was m/z 100—1200 Da, and the 3D data were collected in the continuum mode. The leucine-enkephalin (m/z 556.2771 in positive ion mode) was invoked as the lock mass solution to ensure accurate mass measurement. The MS data were acquired by Waters MassLynx V4.1 software and processed by UNIFI™ 1.8 software (Waters, Milford, MA, USA).

3. Results

3.1. Fragmentation patterns of parent compounds

Generally, the parent drug and related metabolites have the same skeleton, and their fragmentation patterns are similar. In order to make better use of LC-MS technology to analyze metabolites, it is necessary to fully understand the fragmentation behaviors of parent compounds.

The Yanhusuo alkaloids can be mainly classified into the following four types: tetrahydroprotoberberine-type, protoberberine-type, protopine-type and aporphine-type. Tetrahydroberberine and tetrahydropalmatine easily underwent retro-diels alder (RDA) cleavage with complementary fragment ions in MS, since the C-ring was saturated (Figs. S1—S2). Among them, nitrogen-containing fragment ion had the highest abundance. The structure of protopine was similar to that of tetrahydroberberine, which was prone to RDA cleavage (Fig. S3). The fragment ion formed by further dehydration after RDA cleavage was the most abundant. The C-ring of palmatine alkaloid was not saturated, so it

Table 1
The metabolic characteristic fragments (MCFs) of Yanhusuo-derived metabolites.

Type	Standards	MCFs	
		Product ions	Neutral loss (Da)
Tetrahydroprotoberberine alkaloids	Tetrahydroberberine Tetrahydropalmatine	*m/z* 192.1019, *m/z* 178.0869, *m/z* 176.0706, *m/z* 164.0706	$C_6H_8O_6$ (176.0321) SO_3 (79.9568) CH_3 (15.0235) CH_4 (16.0313)
Protopine alkaloids	Protopine	*m/z* 222.1125, *m/z* 208.0968, *m/z* 204.1019, *m/z* 190.0863, *m/z* 206.0812, *m/z* 194.0418, *m/z* 188.0706, *m/z* 176.0706	$C_6H_8O_6$ (176.0321) SO_3 (79.9568) CH_3 (15.0235) CH_4 (16.0313)
Protoberberine alkaloids	Palmatine	$[M-CH_3]^+$ $[M-CH_4]^+$ $[M-C_2H_4O]^+$ $[M-2CH_3]^+$	CH_3 (15.0235) CH_4 (16.0313) C_2H_4O (44.0262)
Aporphine alkaloids	Glaucine	$[M-(CH_3)_2NH]^+$ $[M-CH_3NH_2]^+$	$(CH_3)_2NH$ (45.0578) CH_3NH_2 (31.0344)

was difficult to experience RDA cleavage (Fig. S4). When the substituents contained two or more methoxy groups, the characteristic fragment ions were $[M-CH_3]^+$, $[M-CH_4]^+$, $[M-CH_4-CO]^+$, $[M-2CH_3]^+$ and $[M-CH_3OH]^+$. Owing to the lack of the corresponding reference standards, the fragmentation pattern of aporphine-type alkaloids is summed up by related literature to determine the characteristic fragments [18,19]. A weak bond existed in the amide group, so aporphine-type alkaloids very easily lost $(CH_3)_2NH$ or CH_3NH_2 substituents to produce the most abundant fragment of $[M-45.0578]^+$ or $[M-31.0344]^+$ as the characteristic ions (Fig. S5).

3.2. Study on the metabolism of representative compounds

In order to study metabolites of various components in *Corydalis* comprehensively and systematically, we selected four representative standards, namely, tetrahydroberberine, tetrahydropalmatine, protopine, and palmatine. The metabolites of each compound were identified based on fragmentation patterns of parent compounds

and metabolic pathways summarized from the literature. The metabolic pathways are shown in Fig. 2. As illustrated in this figure, the possible structures of all metabolites were clearly shown, which were not present in previous reports. Compared with those in the literature [11,12,16], new metabolic pathways such as dehydrogenation of tetrahydroberberine and new metabolites like M1-13, M3-7, etc. were also found in this study by the proposed strategy. All metabolites of four representative compounds are listed in Tables S1–S4. Based on the MS information and metabolic pathways summarized from standards, MCFs were proposed to characterize metabolites of Yanhusuo extract (Table 1).

3.3. Establishment of chemical structure screening tables

Notably, it was found that the skeleton of Yanhusuo alkaloids did not change in metabolism. So, the chemical structure screening tables (Tables 2–4) were conducted according to the type and number of substitutes and in vivo metabolic pathways to offer

Table 2
The chemical structure screening table of tetrahydroprotoberberine alkaloids.

[M+H]$^+$	C-2	C-3	C-9	C-10	C-13	Sulfation	Glucuronidation
356.1862	OCH$_3$	OCH$_3$	OCH$_3$	OCH$_3$	H	436.1430	532.2183
370.2018	OCH$_3$	OCH$_3$	OCH$_3$	OCH$_3$	CH$_3$	450.1586	546.2339
340.1549	OCH$_3$	OCH$_3$	-OCH$_2$O-		H	420.1117	516.1870
354.1705	OCH$_3$	OCH$_3$	-OCH$_2$O-		CH$_3$	434.1273	530.2026
342.1705	OCH$_3$	OCH$_3$	OCH$_3$	OH	H	422.1273	518.2026
356.1862	OCH$_3$	OCH$_3$	OCH$_3$	OH	CH$_3$	436.1430	532.2183
342.1705	OCH$_3$	OCH$_3$	OH	OCH$_3$	H	422.1273	518.2026
356.1862	OCH$_3$	OCH$_3$	OH	OCH$_3$	CH$_3$	436.1430	532.2183
328.1549	OCH$_3$	OCH$_3$	OH	OH	H	408.1117	504.1870
342.1705	OCH$_3$	OCH$_3$	OH	OH	CH$_3$	422.1273	518.2026
342.1705	OCH$_3$	OH	OCH$_3$	OCH$_3$	H	422.1273	518.2026
356.1862	OCH$_3$	OH	OCH$_3$	OCH$_3$	CH$_3$	436.1430	532.2183
342.1705	OH	OCH$_3$	OCH$_3$	OCH$_3$	H	422.1273	518.2026
356.1862	OH	OCH$_3$	OCH$_3$	OCH$_3$	CH$_3$	436.1430	532.2183
326.1392	OCH$_3$	OH	-OCH$_2$O-		H	406.0960	502.1713
340.1549	OCH$_3$	OH	-OCH$_2$O-		CH$_3$	420.1117	516.1870
326.1392	OH	OCH$_3$	-OCH$_2$O-		H	406.0960	502.1713
340.1549	OH	OCH$_3$	-OCH$_2$O-		CH$_3$	420.1117	516.1870
328.1549	OCH$_3$	OH	OH	OCH$_3$	H	408.1117	504.1870
342.1705	OCH$_3$	OH	OH	OCH$_3$	CH$_3$	422.1273	518.2026
328.1549	OCH$_3$	OH	OCH$_3$	OH	H	408.1117	504.1870
342.1705	OCH$_3$	OH	OCH$_3$	OH	CH$_3$	422.1273	518.2026
328.1549	OH	OCH$_3$	OH	OCH$_3$	H	408.1117	504.1870
342.1705	OH	OCH$_3$	OH	OCH$_3$	CH$_3$	422.1273	518.2026
328.1549	OH	OCH$_3$	OCH$_3$	OH	H	408.1117	504.1870
342.1705	OH	OCH$_3$	OCH$_3$	OH	CH$_3$	422.1273	518.2026
314.1392	OCH$_3$	OH	OH	OH	H	394.0960	490.1713
328.1549	OCH$_3$	OH	OH	OH	CH$_3$	408.1117	504.1870
314.1392	OH	OCH$_3$	OH	OH	H	394.0960	490.1713
328.1549	OH	OCH$_3$	OH	OH	CH$_3$	408.1117	504.1870
340.1549	-OCH$_2$O-		OCH$_3$	OCH$_3$	H	420.1117	516.1870
354.1705	-OCH$_2$O-		OCH$_3$	OCH$_3$	CH$_3$	434.1273	530.2026
324.1236	-OCH$_2$O-		-OCH$_2$O-		H	404.0804	500.1557
338.1387	-OCH$_2$O-		-OCH$_2$O-		CH$_3$	418.0960	514.1713
326.1392	-OCH$_2$O-		OCH$_3$	OH	H	406.0960	502.1713
340.1549	-OCH$_2$O-		OCH$_3$	OH	CH$_3$	420.1117	516.1870
326.1392	-OCH$_2$O-		OH	OCH$_3$	H	406.0960	502.1713
340.1549	-OCH$_2$O-		OH	OCH$_3$	CH$_3$	420.1117	516.1870
312.1236	-OCH$_2$O-		OH	OH	H	392.0804	488.1557
326.1392	-OCH$_2$O-		OH	OH	CH$_3$	406.0960	502.1713

Red numbers indicated quasi-molecular ions matched with Yanhusuo metabol2ites.

Table 3
The chemical structure screening table of protopine alkaloids.

[M+H]⁺	C-2	C-3	C-9	C-10	C-13	Sulfation	Glucuronidation
386.1967	OCH₃	OCH₃	OCH₃	OCH₃	H	466.1536	562.2288
400.2124	OCH₃	OCH₃	OCH₃	OCH₃	CH₃	480.1692	576.2445
370.1654	OCH₃	OCH₃	-OCH₂O-		H	450.1223	546.1975
384.1811	OCH₃	OCH₃	-OCH₂O-		CH₃	464.1379	560.2132
372.1811	OCH₃	OCH₃	OCH₃	OH	H	452.1379	**548.2132**
386.1967	OCH₃	OCH₃	OCH₃	OH	CH₃	466.1536	562.2288
372.1811	OCH₃	OCH₃	OH	OCH₃	H	452.1379	**548.2132**
386.1967	OCH₃	OCH₃	OH	OCH₃	CH₃	466.1536	562.2288
358.1654	OCH₃	OCH₃	OH	OH	H	**438.1223**	**534.1975**
372.1811	OCH₃	OCH₃	OH	OH	CH₃	452.1379	**548.2132**
372.1811	OCH₃	OH	OCH₃	OCH₃	H	452.1379	**548.2132**
386.1967	OCH₃	OH	OCH₃	OCH₃	CH₃	466.1536	562.2288
372.1811	OH	OCH₃	OCH₃	OCH₃	H	452.1379	**548.2132**
386.1967	OH	OCH₃	OCH₃	OCH₃	CH₃	466.1536	562.2288
356.1498	OCH₃	OH	-OCH₂O-		H	**436.1066**	**532.1819**
370.1654	OCH₃	OH	-OCH₂O-		CH₃	450.1223	546.1975
356.1498	OH	OCH₃	-OCH₂O-		H	**436.1066**	**532.1819**
370.1654	OH	OCH₃	-OCH₂O-		CH₃	450.1223	546.1975
358.1654	OCH₃	OH	OH	OCH₃	H	**438.1223**	**534.1975**
372.1811	OCH₃	OH	OH	OCH₃	CH₃	452.1379	**548.2132**
358.1654	OCH₃	OH	OCH₃	OH	H	**438.1223**	**534.1975**
372.1811	OCH₃	OH	OCH₃	OH	CH₃	452.1379	**548.2132**
358.1654	OH	OCH₃	OH	OCH₃	H	**438.1223**	**534.1975**
372.1811	OH	OCH₃	OH	OCH₃	CH₃	452.1379	**548.2132**
358.1654	OH	OCH₃	OCH₃	OH	H	**438.1223**	**534.1975**
372.1811	OH	OCH₃	OCH₃	OH	CH₃	452.1379	**548.2132**
344.1498	OCH₃	OH	OH	OH	H	**424.1066**	**520.1819**
358.1654	OCH₃	OH	OH	OH	CH₃	**438.1223**	**534.1975**
344.1498	OH	OCH₃	OH	OH	H	**424.1066**	**520.1819**
358.1654	OH	OCH₃	OH	OH	CH₃	**436.1066**	**532.1819**
370.1654	-OCH₂O-		OCH₃	OCH₃	H	450.1223	546.1975
384.1811	-OCH₂O-		OCH₃	OCH₃	CH₃	464.1379	560.2132
354.1341	-OCH₂O-		-OCH₂O-		H	**436.1066**	**532.1819**
368.1498	-OCH₂O-		-OCH₂O-		CH₃	448.1066	544.1819
356.1498	-OCH₂O-		OCH₃	OH	H	**436.1066**	**532.1819**
370.1654	-OCH₂O-		OCH₃	OH	CH₃	450.1223	546.1975
356.1498	-OCH₂O-		OH	OCH₃	H	**436.1066**	**532.1819**
370.1654	-OCH₂O-		OH	OCH₃	CH₃	450.1223	546.1975
342.1341	-OCH₂O-		OH	OH	H	**422.0910**	**518.1662**
342.1341	OH	OH	-OCH₂O-		H	**422.0910**	**518.1662**
356.1498	-OCH₂O-		OH	OH	CH₃	**436.1066**	**532.1819**

Red numbers indicated quasi-molecular ions matched with Yanhusuo metabolites.

Table 4
The chemical structure screening table of protoberberine alkaloids.

$[M+H]^+$	n(OCH$_3$)	n(OH)	n(-OCH$_2$O-)	C-13	Sulfation	Glucuronidation
320.0917	0	0	2	H	400.0491	496.1244
334.1074	0	0	2	CH$_3$	414.0647	510.1400
308.0917	0	2	1	H	388.0491	484.1244
322.1079	0	2	1	CH$_3$	**402.0647**	**498.1400**
296.0917	0	4	0	H	376.0491	472.1244
310.1074	0	4	0	CH$_3$	390.0647	486.1400
310.1074	1	3	0	H	390.0647	486.1400
324.1236	1	3	0	CH$_3$	**404.0804**	**500.1557**
322.1079	1	1	1	H	**402.0647**	**498.1400**
336.1236	1	1	1	CH$_3$	416.0804	512.1557
324.1236	2	2	0	H	**404.0804**	**500.1557**
338.1387	2	2	0	CH$_3$	**418.0960**	514.1713
336.1236	2	0	1	H	416.0804	512.1557
350.1387	2	0	1	CH$_3$	430.0960	526.1713
338.1392	3	1	0	H	**418.0960**	514.1713
352.1543	3	1	0	CH$_3$	**432.1117**	**528.1870**
352.1543	4	0	0	H	**432.1117**	**528.1870**
366.1705	4	0	0	CH$_3$	446.1273	540.1870

Red numbers indicated quasi-molecular ions matched with Yanhusuo metabolites.
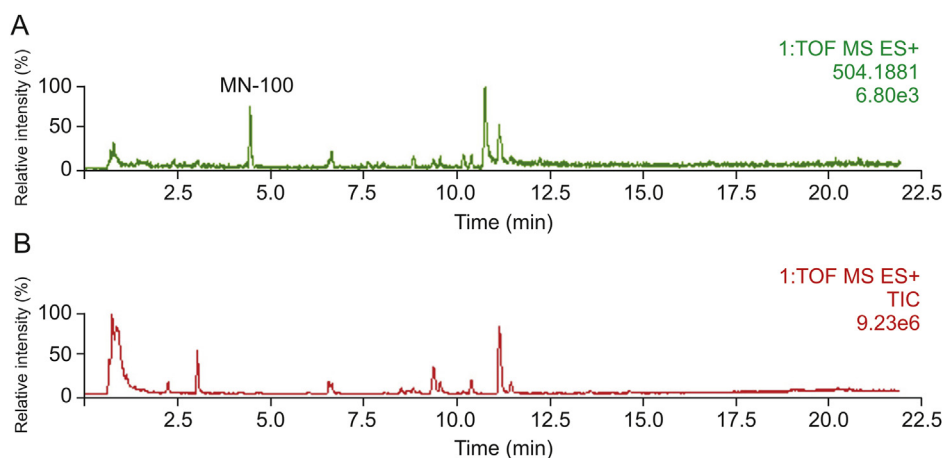
Fig. 3. The chromatograms of clinical Yanhusuo extract administration plasma sample: (A) the extract ion chromatogram of *m/z* 504.1881, and (B) the total ion chromatogram of plasma sample.

references for structure identification.

3.4. Global identification of Yanhusuo-derived compounds

3.4.1. Identification of metabolites detected in preliminary screening

Metabolites with relatively strong MS responses could be detected in preliminary screening based on metabolic characteristic fragments and metabolic pathways. The identification process was illustrated by taking metabolite MN-100 in plasma sample of clinical dose Yanhusuo extract as examples (Fig. 3). The extract ion chromatograms (EIC) of MN-100 is shown in Fig. 3A, and Fig. 3B is the total ion chromatogram of plasma sample. In positive mode, the quasi-molecular ion was *m/z* 504.1881 [M+H]$^+$ and the chemical formula was $C_{25}H_{29}NO_{10}$. The fragment ion *m/z* 328.1548 [M+H]$^+$ suggested that the compound was a glucuronidated
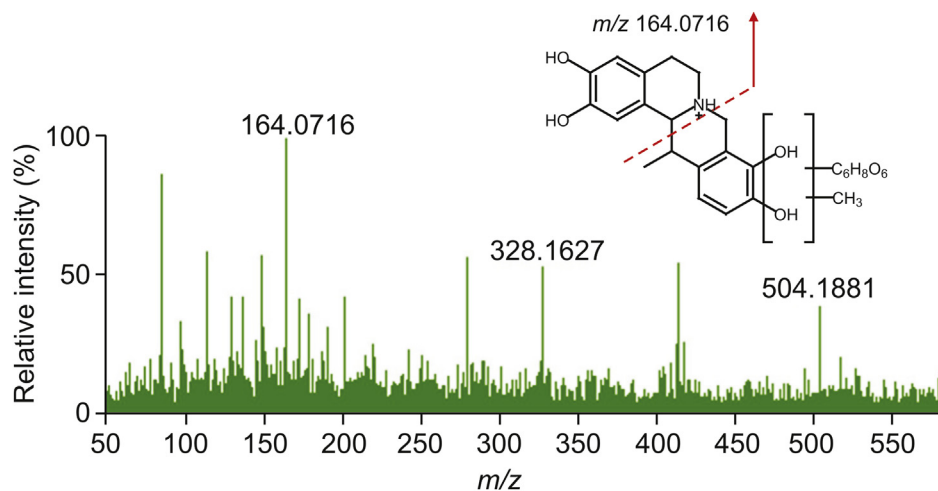
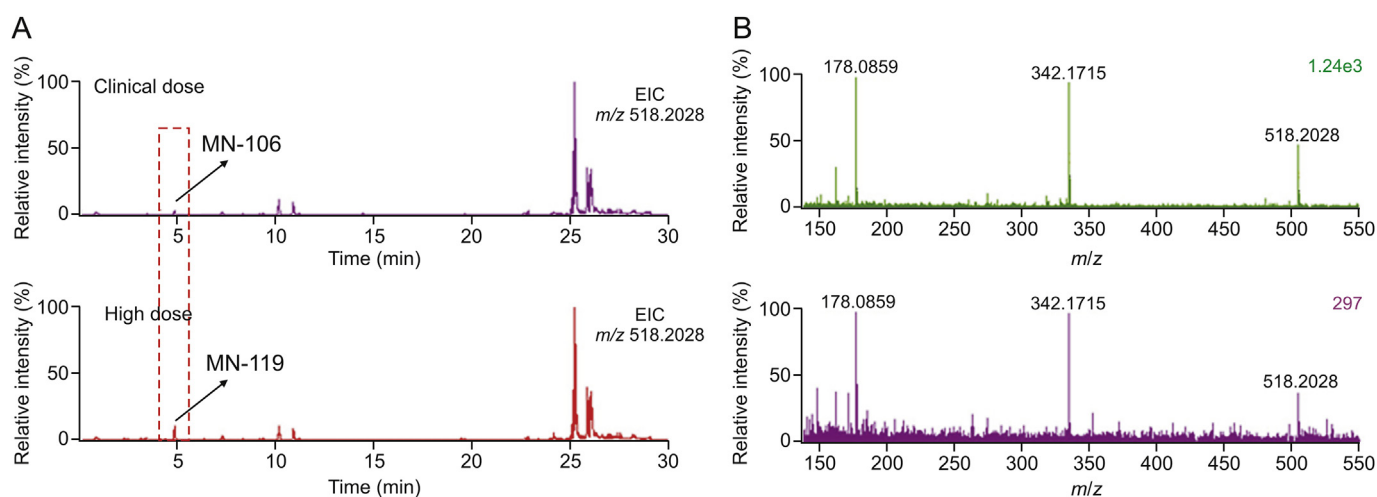Fig. 4. The MS/MS spectra and structure of MN-100.

Fig. 5. The extract ion chromatograms (A) and MS/MS spectra (B) of *m/z* 518.2028 in plasma samples of clinical dose and high dose extracts.

metabolite. The theoretical quasi-molecular ion *m/z* 504.1870 was retrieved in the chemical structure screening tables, corresponding to seven designed metabolite structures (Table 2). These seven metabolites were all tetrahydroprotoberberine-type alkaloids with two or more hydroxyl groups in the structure. The most abundant fragment ion *m/z* 164.0716 indicated the presence of two hydroxyl substitutions on the nitrogen-containing fragment ion produced by RDA cleavage. Therefore, we concluded that the compound had the same skeleton as tetrahydroberberine, with two hydroxyl substitutions at the C2–C3 position, a methyl substitution at the C13 position, and a glucuronic acid and a methoxy group at the C9–C10 position. The MS/MS spectra and structure of MN-100 are shown in Fig. 4.

3.4.2. Identification of metabolites with weak MS responses in the same biological samples from high dose to clinical dose

Some chromatographic peaks were missed in the preliminary screening due to low abundance, poor peak shapes, or inability to

infer structures for lack of MS/MS information. In view of this, we proposed a method using metabolites of high dose Yanhusuo extract as pseudo-standards to identify those of clinical dose. The metabolite MN-106 in Fig. 5A was not detected in preliminary screening due to low abundance and poor peak shape. However, at the same retention time, the metabolite MH-119 in the high dose plasma sample was identified as methylated and glucuronidated tetrahydropalmatine. The EICs of *m/z* 518.2028 in plasma samples of clinical dose and high dose extract are shown in Fig. 5A. It can be seen from the figure that the response of the compound in sample of clinical dose extract was quite low. Partial amplification showed two peaks had the same chromatographic retention behavior. In the MS/MS spectra (Fig. 5B), fragment ions in sample of clinical dose extract had a lower response value, almost submerged in the baseline, but it had the same fragmentation pattern as in sample of high dose, which indicated that MH-119 also existed in sample of clinical dose extract.
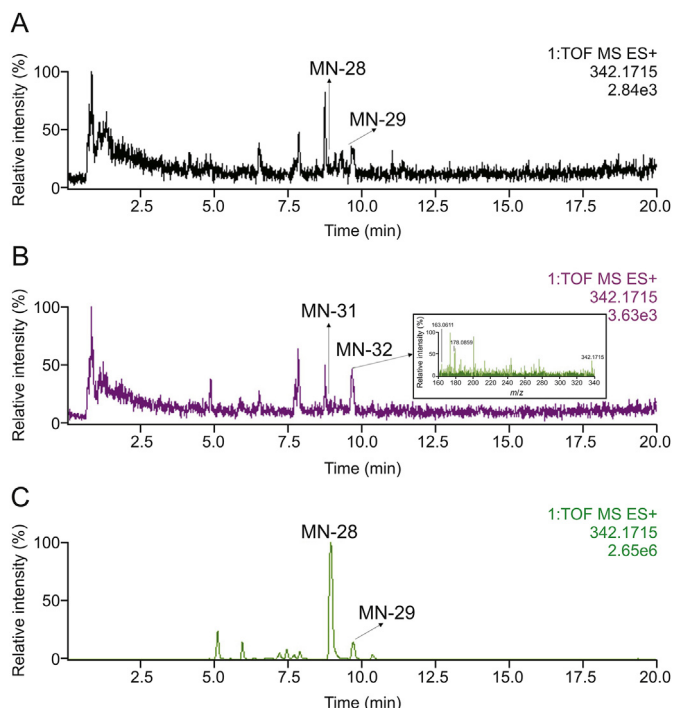
Fig. 6. The extract ion chromatograms of *m/z* 342.1715: (A) clinical dose plasma sample, (B) high dose plasma sample, and (C) clinical dose urine sample.
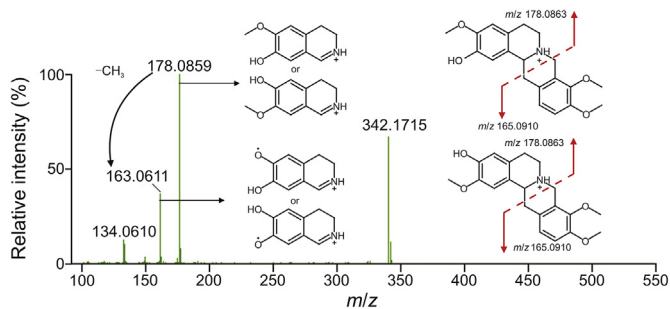

Fig. 7. The MS/MS spectra and structures of MN-28 and MN-29.
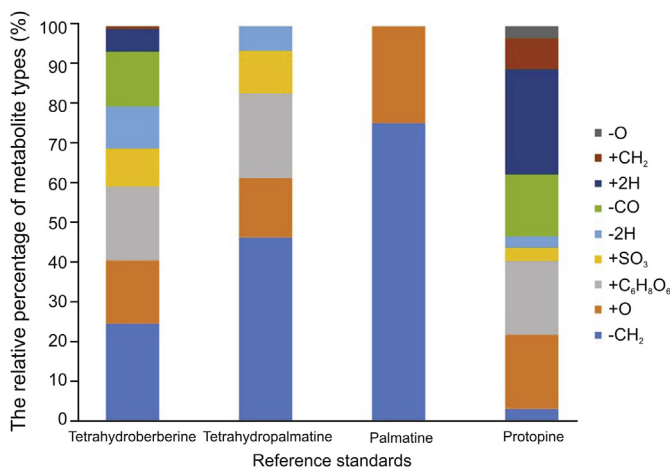

Fig. 8. The relative percentage of metabolite types in four reference standards.

3.4.3. Identification of trace metabolites in the different samples by cross-mapping of different biological samples

The metabolites between the same biological samples obtained at different doses were almost completely coincident, so this method facilitated the identification of metabolites in the same samples. However, biological sample collection and data analysis of different administration doses required a large amount of repetitive work. What's more, high dose Yanhusuo extract did not enhance the MS response intensity of all metabolites. In the data analysis process, we found that there were many overlapping metabolites in different biological samples, while some samples, such as urine and bile, had many kinds of metabolites with high abundance. Thus, metabolites with strong abundance from one sample as pseudo-standards were mapped to all the other three samples correspondingly by retention time and *m/z* value, so trace metabolites in the different samples could be identified. Taking the metabolites MN-28 and MN-29 in plasma samples of clinical dose Yanhusuo as an example, this strategy was illustrated. These two metabolites were not detected in high dose plasma samples during the preliminary screening. As shown in Figs. 6A and B, the MS responses of these two peaks in plasma samples with different doses were very weak, and one peak was even submerged in the baseline. The method from high dose to clinical dose could not identify them from plasma samples, while six metabolites with quasi-molecular ions of *m/z* 342.1715 [M+H]+ were detected in urine sample. In the preliminary screening results of urine sample, the peaks with retention time of 9.05 min and 9.83 min were identified as hydrogenated tetrahydroberberine. Fragment ion at *m/z* 178.0859 [M+H−$C_{10}H_{12}O_2$]+ suggested that the structures of the compounds were similar to those of tetrahydroberberine and the hydrogenated reaction occurred at A or B ring. The theoretical quasi-molecular ion *m/z* 342.1705 was searched in the chemical structure screening tables, and the possible structures were found to be three methoxyl groups and one hydroxyl group at C-2, C-3, C-9, and C-10 of the tetrahydroberberine skeleton. Therefore, hydrogenation occured on the A ring. The structures and MS/MS spectra are shown in Fig. 7. The ion of *m/z* 342.1715 was extracted from the plasma sample, as shown in Figs. 6A and B, to obtain four chromatographic peaks with the same *m/z* values at the same retention time as in urine (Fig. 6C). The mass spectrum of metabolite MH-32 could be amplified locally to find the same fragment ions as those in urine. The other three chromatographic peaks lacked fragment ions but had the same quasi-molecular ions at the same retention time as metabolites in urine and were also identified as metabolites of hydrogenated tetrahydroberberine. The metabolites detected in rat biological samples after oral administration of clinical dose and high dose Yanhusuo extracts can be found in Tables S5–S6. Among them, 127 herb-derived metabolites were identified in rat biological samples after oral administration of clinical dose.

3.4.4. The relationship between structure and metabolism of Yanhusuo alkaloids

In the study of four standards, we found that the structures of Yanhusuo alkaloids were closely related to metabolism. The skeleton of alkaloids did not change during metabolizing. The structure contains many methoxyl groups. Therefore, demethylation was the most common and frequent metabolic reaction. It can be seen from Fig. 8 that palmatine was the most susceptible one to have demethylation at methoxy substitution, followed by tetrahydropalmatine, tetrahydroberberine, and protopine, while the methylation reaction was reversed. The remaining hydroxyl groups were prone to have sulfation and glucuronidation. Both

glucuronidation and sulfation reactions occurred only once and did not occur simultaneously. Only two metabolites were detected to be sulfated twice. The component containing methylenedioxy group would lose one molecule of CO, and the one that did not contain the substituent would not occur the cleavage, as shown in the case of tetrahydropalmatine and palmatine. Five-membered oxygen-containing ring and the carbonyl group of protopine alkaloids were easy to be hydrogenated. The former opened into a methoxyl group and a hydroxyl group, and the latter became a hydroxyl group. The hydroxyl group was unstable and dehydroxylation occurred easily. Dihydroxylation did not happen in other structural types. Protoberberine-type alkaloids did not undergo RDA cleavage due to the unsaturated C ring. So, the structure was difficult to determine and was very stable during the process of metabolism. Palmatine only underwent demethylation and hydroxylation reactions, and metabolites were mainly distributed in feces rather than in bile, suggesting that it might be metabolized by the intestinal tract rather than the liver.

4. Discussion

The in vivo metabolic process of herbal medicine is very complicated, which makes it difficult to explain the mechanism. First, the structures of herbal medicine metabolites were diverse. Compared with previous chemical composition studies in vitro, we found that even though sulfated and glucuronidated metabolites were removed, the structure types of metabolites were more various than that of chemical constituents. In addition, there were still many metabolite isomers, some of which could be distinguished by characteristic fragment ions or ClogP values, but position-isomers or stereo-isomers could not be distinguished by LC-MS data, such as metabolites M4-17, M4-18, M4-19 and M4-20, indicating that more effective methods need to be developed for isomer identification. Second, the metabolic process was complex. Take M4-1 and M4-2 as examples. They were identified as the products of demethylation and dehydroxylation of protopine. This judgment only reflected the final result of element composition change rather than the process. The results of structural identification are shown in Fig. S5. Protopine might experience more complex reactions to produce the metabolites. So, clarifying the structures of metabolites is of great importance for demonstrating the mechanism by which drugs work. Although this study proposed more realistic metabolic pathways based on the identification of metabolite structures, there were still many uncertainties.

5. Conclusions

In this study, 127 metabolites were detected from rat biological samples of clinical dose of Yanhusuo extract using the cross-mapping of different samples and doses, and the strategy from representative standards to herbal extracts and from high dose to clinical dose of herbal extracts. What's more, the chemical structure screening tables were combined with characteristic fragment ions to clarify the metabolite structures. More accurate metabolic pathways of four representative standards in rats were drawn, and the relationship between structure and metabolism of Yanhusuo alkaloids was demonstrated. Thus, this strategy had advantages in herb-derived metabolites research. It solved problems like the high response of biological samples matrix, low metabolite concentration, inconspicuous peak shape, and absence of MS/MS information, which caused barriers in structure identification of

metabolites. Structural types of metabolites that are more abundant than in vitro chemical components and clear in vivo metabolic pathways will be a great help for finding bioactive components of Yanhusuo. The strategy proposed in this study will be a powerful tool in the discovery of pharmacodynamic substances and metabolic mechanism research.

Declaration of competing interest

The authors declare that there are no conflicts of interest.

Appendix A. Supplementary data

Supplementary data to this article can be found online at https://doi.org/10.1016/j.jpha.2020.03.006.

References

[1] G.F. Feng, Y.F. Sun, S. Liu, et al., Stepwise targeted matching strategy from *in vitro* to *in vivo* based on ultra–high performance liquid chromatography tandem mass spectrometry technology to quickly identify and screen pharmacodynamic constituents, Talanta 194 (2019) 619–626.

[2] S.T. Yu, H.X. Liu, K. Li, et al., Rapid characterization of the absorbed constituents in rat serum after oral administration and action mechanism of Naozhenning granule using LC-MS and network pharmacology, J. Pharmaceut. Biomed. Anal. 166 (2019) 281–290.

[3] H.Y. Zhang, S.R. Duan, L. Wang, et al., Identification of the absorbed components and their metabolites of Tianma-Gouteng granule in rat plasma and bile using ultra-high-performance liquid chromatography combined with quadrupole time-of-flight mass spectrometry, Biomed. Chromatogr. 33 (2019), e4480.

[4] W. Zhou, J.J. Shan, M.X. Meng, A two-step UPLC-Q-Tof/MS with mass defect filtering method for rapid identification of analogues from known components of different chemical structure types in *Fructus Gardeniae - fructus Forsythiae* herb pair extract and in rat's blood, J. Chromatogr. A 1563 (2018) 99–123.

[5] M.Y. Liu, S.H. Zhao, Z.Q. Wang, et al., Identification of metabolites of deoxyschizandrin in rats by UPLC-Q-TOF-MS/MS based on multiple mass defect filter data acquisition and multiple data processing techniques, J. Chromatogr. B 949–950 (2014) 115–126.

[6] Y. Xu, Q. Wang, Z.H. Yin, et al., On-line incubation and real-time detection by ultra-performance liquid chromatography-quadrupole time-of-flight mass spectrometry for rapidly analyzing metabolites of anthraquinones in rat liver microsomes, J. Chromatogr. A 1571 (2018) 94–106.

[7] Z.H. Huang, Y. Xu, Q. Wang, Metabolism and mutual biotransformations of anthraquinones and anthrones in rhubarb by human intestinal flora using UPLC-Q-TOF/MS, J. Chromatogr. B 1104 (2018) 59–66.

[8] Y. Luo, C.J.S. Lai, J. Zhang, et al., Comprehensive metabolic profile of phenolic acids and flavonoids in Glechomae Herba using ultra-high-performance liquid chromatography coupled to quadrupole-time-of-flight tandem mass spectrometry with diagnostic ion filtering strategy, J. Pharmaceut. Biomed. Anal. 164 (2019) 615–629.

[9] N. Mi, T.F. Cheng, H.L. Li, et al., Metabolite profiling of traditional Chinese medicine formula Dan Zhi Tablet: an integrated strategy based on UPLC-QTOF/MS combined with multivariate statistical analysis, J. Pharmaceut. Biomed. Anal. 164 (2019) 70–85.

[10] Chinese Pharmacopoeia Commission, Pharmacopoeia of the People's Republic of China, Chinese Medical Science and Technology Press, Beijing, 2015, pp. 139–140.

[11] W.H. Wang, J. Liu, X.N. Zhao, et al., Simultaneous determination of *L*-tetrahydropalmatine and its active metabolites in rat plasma by a sensitive ultra-high-performance liquid chromatography with tandem mass spectrometry method and its application in a pharmacokinetic study, Biomed. Chromatogr. 31 (2016), e3903.

[12] W.B. Xiao, G.L. Shen, X.M. Zhuang, et al., Characterization of human metabolism and disposition of levo-tetrahydropalmatine: qualitative and quantitative determination of oxidative and conjugated metabolites, J. Pharmaceut. Biomed. Anal. 128 (2016) 371–381.

[13] H.Y. Ji, H. Lee, J.H. Kim, et al., *In vitro* metabolism of corydaline in human liver microsomes and hepatocytes using liquid chromatography-ion trap mass spectrometry, J. Separ. Sci. 35 (2012) 1102–1109.

[14] L.W. Chai, P.O. Donkor, K. Wang, et al., Metabolic profiles of corydaline in rats by ultra-performance liquid chromatography coupled to quadrupole time-of-flight mass spectrometry, Xenobiotica 49 (2019) 80–89.

[15] K.T. Li, Pharmacokinetics and metabolism of quaternary protoberberine

alkaloids of *Corydalis Yanhusuo* [master's thesis], Peking Union Medical College, Beijing, 2012.

[16] K. Wang, L.W. Chai, L.Q. Ding, et al., Identification of metabolites of palmatine in rats after oral administration using ultra-high-performance liquid chromatography/quadrupole time-of-flight mass spectrometry, Rapid Commun. Mass Spectrom. 31 (2017) 523–537.

[17] F.R. Miao, G.Y. Liu, L. Lin, Constituents absorbed in rat serum after oral administration of Rhizoma Corydalis extraction with HPLC-MS-MS, Chin. J. Exp. Tradit. Med. Formulae 19 (2013) 166–170.

[18] M.L. Wang, Y.H. Liu, S. Fu, et al., Applying target data screening followed by characteristic fragment filtering for the comprehensive screening and identification of alkaloids in *Corydalis yanhusuo* W.T. Wang by UPLC-Q-TOF/MS^{E}, RSC Adv. 7 (2017) 53545–53551.

[19] J. Schmidt, C. Boettcher, C. Kuhnt, et al., Poppy alkaloid profiling by electrospray tandem mass spectrometry and electrospray FT-ICR mass spectrometry after [ring-^{13}C$_6$]-tyramine feeding, Phytochemistry 68 (2007) 189–202.